

LAGOON WATER-LEVEL OSCILLATIONS DRIVEN BY RAINFALL AND WAVE CLIMATE

González-Villanueva, R.^{1,2}, Pérez-Arlucea, M.¹ and Costas, S.³

¹ Departamento de Xeociencias Mariñas e O.T. (XM1), Universidade de Vigo, 36310 Vigo, Spain

² Department of Geography, University of Dundee, Dundee, Scotland

³ CIMA, Universidade do Algarve, Portugal Campus de Gambelas, Edifício 7, 8005-139 Faro,
Portugal

Corresponding author: González-Villanueva R. ritagonzalez@uvigo.es

ABSTRACT

Barrier breaching and subsequent inlet formation represent critical processes that ensure the temporary or permanent connection and transference of water, nutrients, or living organisms between a lagoon and the open sea. Here, we investigate the conditions inducing natural barrier breaching through a 34 months monitoring program of water-level oscillations within a shallow lagoon and the adjacent nearshore, at the Northern coast of the Iberian Peninsula, Louro lagoon. Seven natural openings were identified during the three monitored wet seasons (Wet1, Wet2 and Wet3), four in the Wet1, two in the Wet2 and 1 in the Wet3. Identified openings were grouped in three types depending on the observed relation between the lagoon water-level (L_{wl}), the berm height (B_h) and the water-level at the beach (B_{wl}): (i) openings by lagoon outflow, which include those characterized by L_{wl} higher than the B_h and lower B_{wl} ; (ii) openings by wave overwash, including those induced by B_{wl} higher than the B_h , and (iii) mixed openings, which result from a combination of the two previous conditions. We have found that the L_{wl} is modulated by the rainfall regime (R_f) and can be explained by the accumulated precipitation while B_h and B_{wl} depend on the wave climate and tidal level and can be estimated applying runup equations. The inlet lifespan was found to be regulated by the wave climate and rainfall regime; in particular barrier sealing was associated with a sudden increase in wave period and reduction in precipitation. This work proves that the natural openings could be predicted successfully with support to medium term water-level monitoring programs, which in turn may significantly contribute to strategic decision making for management and conservation purposes.

KEYWORDS

Natural barrier breaching, rainfall regime, wave climate, coastal lagoon, berm height, tidal range, intermittent inlet

1. INTRODUCTION

Coastal barrier breaching (inlet formation) is a complex morphodynamic process that enables free water exchange between the lagoon and the open sea. Processes performing at both the seaward and the bay side of a barrier may induced barrier breaching (Boothroyd, 1985; Fagherazzi and Priestas, 2012; Gordon, 1990; Hayes, 1979; Kraus et al., 2002; Pierce, 1970). The consequences of such processes are not restricted to lagoon and barrier morphology (Bird, 1993; FitzGerald et al., 2000; Gordon, 1990; Kraus et al., 2002; Morris and Turner, 2010; Pacheco et al., 2011), but they also have a significant impact over the biogeochemical fluxes by promoting water, sediments, nutrients and pollutants exchange, with the sea (Dussaillant et al., 2009; Dye and Barros, 2005; Gale et al., 2006; Moreno et al., 2010; Schallenberg et al., 2010). Once open, inlets can remain active or close after a period of time depending on their hydraulic efficiency, which in turn depends on the rainfall regime, the tidal prism and the long-shore and/or cross-shore sediment transport by local waves (Castelle et al., 2007; Cayocca, 2001; Cruces et al., 2009; Fitzgerald et al., 1984; Fortunato et al., 2014; Green et al., 2013; Ranasinghe and Pattiaratchi, 2003; Ranasinghe et al., 1999; Rich and Keller, 2013). Yet, inlets can intermittently open and close, imposing a temporary character to the connection between lagoons and the ocean.

Depending on the timing of their opening through the year, inlets can be regular, i.e. the connection with open sea occurs seasonally or cyclically, or they can be irregular, if the opening timing does not occur periodically. Regular openings are related to seasonal favorable conditions such as (i) high water-levels and large storm waves impacting the sea side of coastal barriers, or (ii) lagoon high water-levels induced by strong river discharges and heavy rainfalls (Bird, 1993; Dussaillant et al., 2009; Gale et al., 2006; Gordon, 1990; Weidman and Ebert, 2013). Alternatively, irregular openings usually occur at sites where the seasonal contrasts are not significant, preventing periodic timing in their opening-closing behavior (Gale et al., 2006; Gordon, 1990; Morris and Turner, 2010). Yet, it is worth noticing that many of the examples described in the literature refer to manually opened inlets (with the support of bulldozers) for flood-abatement and flushing purposes (Fortunato et al., 2014; Kraus and Wamsley, 2003; Roy et al., 2001; Wainwright and Baldock, 2015).

Establishing the frequency and the thresholds of natural barrier breaching and closure is crucial for

vulnerability assessment and to prevent the loss of human lives, damage to infrastructures in populated coastal areas and/or damage to ecosystem services. Despite this, understanding barrier breaching and closure is constrained by limitations related to the apparently unpredictable character of natural openings and closures, and the oftentimes lack of data regarding barrier breaching and inlet development fronting a coastal lagoon. Indeed, very few are the examples that include a complete monitoring to understand all the processes involved and provide the required information for management purposes.

To our knowledge, so far only a few studies have been made in small coastal lagoons -pocket lagoons- (Figueiredo et al., 2007; Gordon, 1981; Rijkenberg, 2015), and are inexistent in coastal lagoons located in rocky coasts. In this regard, the present work aims at resolving the mechanisms behind barrier breaching and closure of intermittently connected lagoons by monitoring water-levels in a coastal lagoon. The study site is located at the NW Iberian coast, with a relatively small surface and catchment area and feeding by an ephemeral river. The aim is to improve our understanding on natural breaching and closure processes with particular attention to those openings induced by extremely high water lagoon levels. To understand the mechanisms behind the opening and closure of the ephemeral inlet at Louro lagoon we have examined the water-level changes in the lagoon and explored the most likely associated forcers. This was undertaken through the analysis of different data sets of water-level monitoring (sea and lagoon), topographic, wave climate and meteorological data.

2. STUDY SITE

The explored pocket coastal lagoon (*Louro*) is located in a small embayment at the northern margin of the *Ría de Muros* entrance, at the Atlantic coast of Galicia, NW Iberia (Figure 1). Louro lagoon is a pocket lagoon and is influenced by both fresh and saline waters (Cobelo-García et al., 2012). It is an important habitat for numerous plant and animal species, and is included in the Natura 2000 network of the European Union (EU).

The lagoon is a very shallow water body with a flat bottom bed (Figure 1). It has a surface area about 0.25 km², nearly 0.62 km-long and around 0.34 km wide. Reed beds characterize the marginal areas of the lagoon, where the sediment is mostly sand and silt. Sandy sediments characterize the central area, while muddy sediments dominate the inland sector. The communication with the open sea usually

happens through barrier breaching and inlet formation during winter. The inlet opens at the westernmost part of the lagoon (Figure 1D). A 2 m-depth channel with an average width of 15 m cuts the barrier perpendicular to the shoreline just after the barrier is breached (González-Villanueva, 2013; Pérez-Arlucea et al., 2011). Over time, the channel shifts to the north with its long axis becoming parallel to the shoreline until its closure (Almécija, 2009).

The lagoon is separated from the open sea by a 300-600 m-wide and 1500 m-long sand barrier, which anchors to rocky outcrops at both ends (Figure 1). The sandy barrier hosts a dune ridge fragmented by aeolian corridors running across the dune from the upper part of the beach. The dune-ridge reaches maximum heights of 15 m above the Mean Sea-Level in Alicante (MSLA; topographic Spanish Zero, located 1.893 m above mean sea level at Coruña maritime port; see www.puertos.es for more information). High waves come from W to NW directions, with higher values (more than 8 m) during winter (Figure 1C). The NW-SE orientation of the system protects the barrier from the direct impact of these energetic waves. The beach morphology oscillates between two morphodynamic states i.e., intermediate and reflective morphologies from summer to winter conditions respectively (Almécija et al., 2009). In addition, Almécija et al. (2009) demonstrated that the presence offshore of a shallow zone provokes changes in the wave approaching to the coast and a wave divergence with an important energy loss in the northern area of the sand barrier.

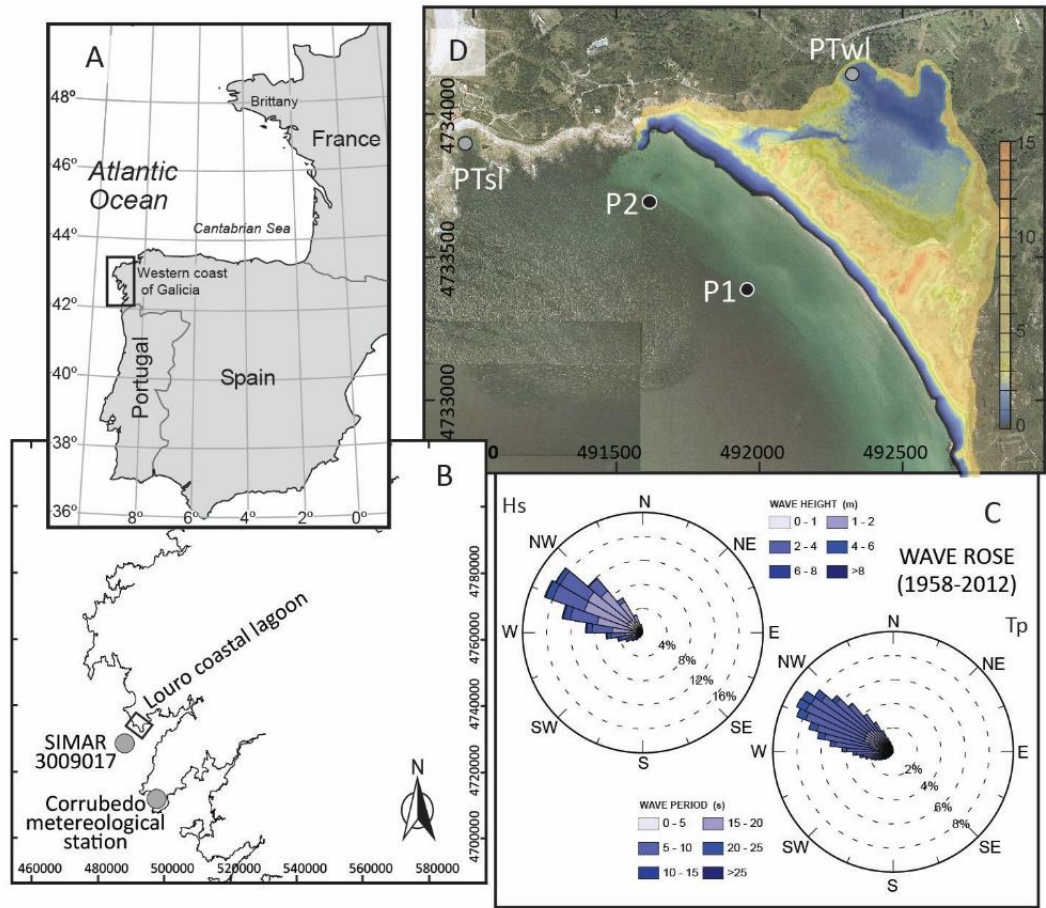


Figure 1. Location of field site. (A): Location in the framework of the Iberian Peninsula. (B): Position of Louro coastal lagoon, SIMAR node and meteorological station. (C): Significant wave height (H_s) and period (T_p), at SIMAR 3009017 point. (D): Aerial imagery of Louro coastal barrier lagoon (2004), with MDT of the barrier and lagoon derived from LiDAR data (2009). The grey dots indicate the location of the water-level loggers. PTsl: sea level record; PTwl: lagoon record; P1 and P2 are the locations for the points used to extract wave characteristics from SWAN propagation model.

Water-level oscillations within the lagoon are mostly seasonal and related to catchment runoff (Cobelo-García et al., 2012; González-Villanueva, 2013; Pérez-Arlucea et al., 2011). Louro catchment area is 4.57 km², with a mean basin slope of 0.19 m/m. The areal percentage of plutonic rocks in the catchment area is 12.58 %, metamorphic rocks 18.83 % and sedimentary (quaternary) rocks and soil 68.59 %. Natural scrubland, abandoned agricultural plots and sparse trees complete the landscape of the catchment areas. The drainage network has a marked torrential regime except for the main tributary, which is the only one with a seasonal water discharge, despite its reduced flow distance of 3.85 km.

Louro is located at the southern limit of the North Atlantic storm track. This region is particularly sensitive to interannual shifts in the trajectories of the mid-latitude cyclones, which are controlled by

the North Atlantic Oscillation -NAO- (Goodess and Jones, 2002; Osborn et al., 1999). The rainfall in the study area is highly variable, with an average rainfall ranging from 600-700 mm in winter to less than 100 mm in summer. The average annual rainfall is close to 1700 mm (Martínez Cortizas and Pérez Alberti, 1999). Previous works suggested that precipitation in this region is strongly modulated by the NAO, with more humid conditions during winters corresponding to low and negative NAO index values (Rodríguez-Fonseca and de Castro, 2002; Trigo et al., 2008).

3. MATERIAL AND METHODS

Two water-level loggers were deployed at the study site to monitor water-level oscillations (Figure 1, Table 1). Available topographic data (Table 1) was obtained from two high-resolution DTMs, measured at low and high lagoon water-levels. These data were used to examine the morphology of the barrier and the bottom topography of the lagoon. The first was surveyed on 19/09/2009, with a Terrestrial Laser Scanner (TLS) Class-1 TSL-RIEGL model LMS Z-390i while the second was surveyed by the IGN on 8/03/2011 using an airborne LiDAR (downloaded from <http://pnoa.ign.es/coberturalidar>). The DTM were constructed based on the Geodetic Reference System ED50 and were represented on the UTM mapping projection (UTM zone 29N). All heights were referred to MSLA.

Metoccean data were also examined and jointly analyzed with in-situ water levels: (i) meteorological data (i.e. rainfall and evaporation parameters) from a near coastal meteorological station -Corrubedo station (Figure 1) - (downloaded from <http://www.meteogalicia.gal/web/index.action>), and (ii) wave climate data from one node of the SIMAR dataset (courtesy of Puertos del Estado), which includes hindcast winds, sea-level and waves starting in 1958 (Figure 1, Table 1).

Table 1. Summary of the available data.

Available data				
Type of data	Units	Temporal resolution or accuracy	Temporal range	Data source
Rainfall	l/m ²	10 min mean	10/2009-7/2012	Meteogalicia
Evaporation	l/m ²	24 hour mean	10/2009-7/2012	Meteogalicia
Offshore waves (H, T, Direction)	(m, s, °)	3 hour mean	10/2009-12/2011	Puertos del Estado
		1 hour mean	12/2011-7/2012	
Sea level	M	5 min mean	10/2009-1/2012	Survey-Pressure transducer
Lagoon water-level	M	5 min mean	10/2009-7/2012	Survey-Pressure transducer
DTM's	M	H: 3mm V:3mm	19/09/2009	Survey-TLS
Topographic data	M	H: 8mm V:15mm	30/01/2010	Survey- DGPS-RTK
Topographic data	M	H: 8mm V:15mm	05/02/2010	Survey-DGPS-RTK
DTM's	M	H: 0.15m V:0.2m	08/03/2011	LiDAR- IGN
Topographic data	M	H: 8mm V:15mm	29/09/2011	Survey-DGPS-RTK

3.1. Lagoon water-level changes

3.1.1. Lagoon water-level monitoring

One logger was located in the lagoon to register lagoon water-levels (L_{wl} ; Figure 1). Water oscillations were recorded at 5 min time intervals, for 34 months (Table 1) with Water-level logger models Seabird SBE 39 and AQUALogger 520 PT. The elevation of the logger was measured, once deployed, using a Trimble DGPS-RTK. Observations were therefore referred to the MSLA by referencing to the corresponding water logger elevation. Water-level measurements were corrected for variations in barometric pressure using the data downloaded from the closest meteorological station (Figure 1).

Corrected data were used to determine the timing of lagoon natural opening, the duration of the active inlet phase, inlet sealing and the associated water-level thresholds. In addition, these data allowed us to identify the parameters that can characterize the lagoon openings: (i) the plateau phase, which corresponds to the time (in hours) between the moment when the lagoon reaches its highest water-level and the breach, and (ii) the water-head (or hydraulic head) difference (in meters), which was calculated as the difference between the lagoon water-level and the water-level in the nearshore at the opening.

3.1.2. Rainfall regime impact on lagoon water-level

The relation between L_{wl} and the rainfall was evaluated using the accumulated rainfall (R_f) for the periods when the lagoon was closed. First the periods with more intense and frequent rainfalls or wet seasons were identified, including also the periods during which the lagoon opens. In addition, the water storage capacity of the lagoon was obtained using the bathymetry to translate lagoon water-levels into water-volumes (L_v). Therefore, the relation between L_v and R_f was obtained, which can be applied for

any situation knowing the accumulated rainfall. In addition, the obtained expression can only be applied after a certain level in the lagoon is reached in order to allow direct comparison between events (L_{mwl}). To select the latter, we have imposed criteria to normalize all the data that is defined by local sea water levels:

$$(1) L_{mwl} = MW + \frac{1}{2} (MHW - MW)$$

where MW is sea mean water-level and MHW is the high sea mean water-level

3.2. Nearshore water-levels

3.2.1. Tidal regime

The tidal regime was monitored using a logger located at the beach nearshore (Figure 1). Water oscillations at the nearshore were recorded at 5 min time intervals, for 28 months (Table 1). We used the same models of water-level loggers as previously described for the L_{wl} monitoring. The same topographic and barometric corrections used for the lagoon water-level record were applied to these data. The corrected record was analyzed using the script World Tides (Boon, 2004) for MATLAB software. This MATLAB routine calculates the tidal curves and residuals (storm surges) using the highest astronomical tide (HAT) and the lowest astronomical tide (LAT). Different reference tidal-levels were obtained from the data record: MW, MHW and mean low water-level (MLW). Identified short gaps in the observed sea-level record due to failures in the logger were corrected by including the predicted tide level obtained with the same MATLAB routine. The tidal height (T_h) at identified lagoon openings were extracted from the record.

3.2.2. Runup

The runup formulation (equation 2) proposed by Stockdon et al. (2006) was chosen to estimate the 2% exceedance value of runup peaks (R_2). Among the available formulas for runup calculation, this one was selected because can be applied to intermediate or reflective beaches. Indeed, under storm conditions (reflective beaches, with $\xi_0 > 1.25$), where the swash is dominated by incident energy, the equation 2 can be simplified into the equation 3.

$$(2) R_2 = 1.1 \left(0.35 \beta_f \sqrt{(H_0 L_0)} + \frac{\sqrt{[H_0 L_0 (0.563 \beta_f^2 + 0.004)]}}{2} \right) \text{ or } (3) R_2 = 0.73 \beta_f \sqrt{(H_0 L_0)}; \text{ for } \xi_0 > 1.25$$

where β_f is the beach-face slope, H_0 and L_0 are the deep-water wave height and length, respectively. The ξ_0 is a non-dimensional surf similarity parameter or Iribarren number (Battjes, 1974) and is defined by the equation 4:

$$(4) \quad \xi_0 = \frac{\beta_f}{\sqrt{(H_0 L_0)}}$$

The beach morphology falls into the reflective type during winter conditions (Almécija, 2009) with an average winter slope of 0.1, which was used to calculate the Iribarren number and the runup values. B_{wl} at the breaching moment was obtained by the addition of the measured tidal-level (T_h) and the calculated runup levels (R_2).

To estimate runup levels at the beach we have used the wave data from a hindcast time series extracted from the SIMAR-3009017 node, located offshore of Louro (Figure 1), for the time period overlapping the record of the water loggers. Because of the orientation and irregular shape of the coast, offshore waves have been propagated onshore using a bathymetric grid with the best available data with a 50m resolution. The SIMAR wave data were used to feed the SWAN (Simulating Waves Nearshore) model (Booij et al., 1999) to simulate the nearshore wave climate. The model was run in non-stationary mode using one computational grid based on the bathymetric grid and was forced along its open boundaries by the integral parameters of the wave time series: H_s , T_p and θ_p . The spectral domain was discretized with 31 frequency bins (distributed logarithmically between 0.04 and 1), with a directional spreading coefficient of 3. Wave parameters (H_s , T_p and θ_p) were extracted from 2 locations alongshore the Louro embayment at 12 m depth (Figure 1).

To ensure the correct application of equation 2, the simulated nearshore waves were reversed shoaled to deep-water using the linear wave theory, and assuming a shore-normal approach and the unrefracted wave height and period as suggested by Stockdon et al. (2006).

A similar approach was used to estimate a range in the elevation of the sandy barrier ($B_{hmin} - B_{hmax}$) by assuming that B_{wl} during antecedent spring-high tides is a proxy for beach berm elevation. The latter is in turn assumed as representative of the barrier dimensions at the area where the barrier breaches, which in turn lacks any dune building.

4. RESULTS

4.1. Lagoon water-levels

Figure 2A shows the water-level in the lagoon. The basal lagoon water-level was around 2 m (MSLA), which was reached during the dry seasons and when the lagoon was opened. In general terms, when the wet season starts, L_{wl} gradually raises 2 m, reaching values above 4 m MSLA (Figure 2A). All recorded openings at Louro were natural; they had not been artificially forced or initiated. Opening events were easily recognized within the lagoon water-level record as sharp elevation drops (1-2 m), occurring in a short period of time (8-12 hours). The maximum level recorded in the lagoon before barrier breaching was 4.72 m in March 2010 (Figure 2A, Table 2-event 3-). However, the maximum water-level recorded in the lagoon was 4.83 m in February 2011 (Figure 2A-star-, Table 2-event *-), which did not trigger a breaching but showed a gradual water-level lowering that spanned over few months in the following spring and summer.

When breaching occurs, and the lagoon communication opens, water fluctuations driven by tides are propagated inside the lagoon, showing a small time lag relative to the nearshore water-level (Figure 2A). The number of days that the lagoon remained open ranged between 7 and 29 days (Table 2). Once the connection with the open sea became more restricted, tidal fluctuations in the lagoon were flattened, tending to disappear.

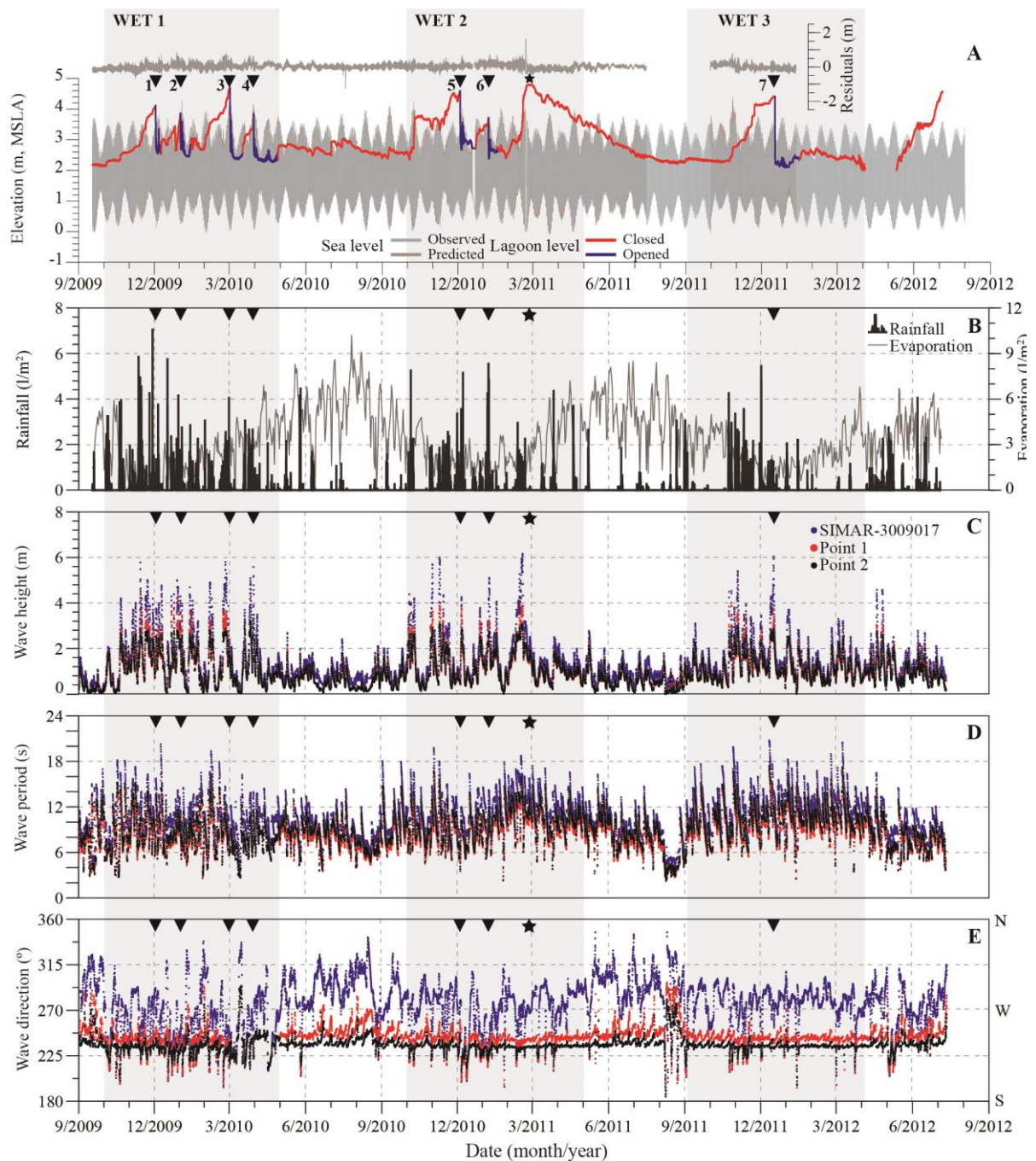


Figure 2. (A) Water-levels obtained from the loggers: observed, predicted and residual sea-level and water oscillations in the lagoon (red close and blue open). (B) Rainfall and evaporation record from the Corrubedo meteorological station during the same period. Grey bands show the wet seasons 1 to 3 (October to April) during the test period. Black arrows indicate the most significant events of inlet opening: 1 to 7. Star symbol corresponds to high water-levels in the lagoon which not ended in a barrier breaching. (C,D,E) Wave height (m), period (s) and direction (°) record of offshore waves obtained from the SIMAR node and at the points 1 and 2 from the SWAN model.

Table 2. Detailed information of water-levels into the lagoon, rainfall, tides and waves for opening events. Initial water-levels in the lagoon are established as the minimal water-level before a breach (L_{mwI}). Beach berm values (minimal and maximum) are calculated by adding to the height of the spring-high tides values the corresponding runup values before a barrier beach. The plateau phase corresponds to the time (in hours) between the highest water-level reached by in the lagoon and the breach. The barrier recovery time is referred to the time between the closing of the inlet. The next opening is given in days. The water-head (or hydraulic head) difference (in meters) was calculated as the difference between the water-level in the lagoon and in the barrier. Accumulated rainfall corresponds to the rainfall drop lapsing between the moments that the lagoon reaches the L_{mwI} and a barrier breaching event. The event marked as * corresponds with a maximum water-level not leading to an opening. Different font colors in the events correspond to different wet seasons.

Event	Lagoon water-level (m)/Date		B_{hmin} - B_{hmax} (m)	Plateau phase (h)	Days open	Barrier recovery time (days)	Characteristics at barrier breaching								
	Initial level (m)	Breach level (m)					Water- head (m)	Accumulated rainfall (l/m ²)	Water- level at the beach (m)	Wave direction (°)	Wave height (m)	Tidal level (m)	Tidal stage	Tidal type	Tidal range (m)
1	2.91 (14/11/2009)	4.14 (2/12/2009)	4.1-5.1	15.5	7	>76	-0.19	153	4.33	239-WSW	1.52	3.13	Rising, close to high	Close spring	2.98
2	2.91 (28/12/2009)	3.89 (1/1/2010)	3.9-4.1	5.8	13	4	0.83	40.8	3.06	242-WSW	2.57	1.38	Falling, close to low	Spring	3.73
3	2.91 (31/1/2010)	4.72 (2/3/2010)	4.2- 5.1	21.8	15	48	1.09	162.1	3.63	232-SW	1.17	2.80	Rising, close to high	Spring	4.11
4	2.91 (18/3/2010)	3.49 (30/3/2010)	3.7-4.8	---	29	13	-2.03	78.5	5.51	231-SW	2.57	3.49	Close high	Spring	4.29
5	2.91 (8/10/2010)	4.62 (3/12/2010)	4.6- 4.8	46.3	13	229	2.93	261.6	1.69	239-WSW	0.64	1.05	Falling close to low	Close spring	2.55
6	2.91 (22/12/2010)	3.57 (6/1/2011)	4.5-4.8	---	11	19	-1.28	81.1	4.84	223-SW	2.23	3.55	Rising, close to high	Spring	3.07
*	2.91 (3/2/2011)	4.83* (25/2/2011)	5.2-5.3	153	---	---	1.15*	105.9	3.68*	230*-SW	1.19*	2.48*	Rising*	Neap*	1.65
7	2.91 (3/11/2011)	4.43 (16/12/2011)	4.2-5.1	61.2	20	344	1.13	265.8	3.30	233-SW	2.78	1.3	Low	Close neap	2.12

4.2. Impact of rainfall on lagoon water-levels

Figure 2B shows rainfall and evaporation data for the same time interval. From these data, we could identify three wet seasons during the monitoring program: Wet1 extended from October 2009 to April 2010, Wet2 from October 2010 to April 2011, and Wet3 between October 2011 and April 2012. The total rainfall decreased from Wet1 to Wet3. Seven opening events were identified; 4 events during Wet1, 2 events during Wet2, and only one event during Wet3. The first opening event of each wet season was characterized by L_{wl} above 4 m (Table 2) while consecutive openings within a same season were below 4 m, which means that the time interval for barrier recovery would be relatively short; openings 2, 4 and 6 (Table 2).

Figure 3A shows the relationship between L_{wl} and the corresponding L_v for L_{wl} higher than 2.91 m (L_{mwl} obtained using equation 1). The relation (with a r^2 value of 0.99) between these variables was:

$$(4) L_v = 259641L_{wl} - 643018$$

Figure 3B shows L_v versus R_f for each opening event between the moments in which the imposed criteria is attained ($L_{wl}=L_{mwl}$) and the breaching moment. The relation (with a r^2 value of 0.75) between these variables can be described with by the following regression:

$$(5) L_v = 1211R_f + 1.77e^{+05}$$

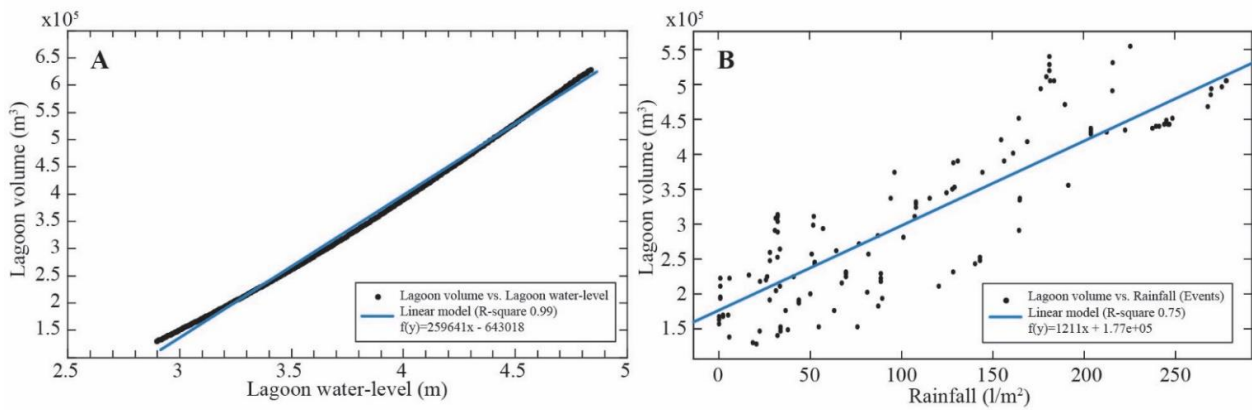


Figure 3. (A) Lagoon water volume in m^3 versus lagoon water-level in m (black points) and the linear regression (blue line) **(B)** Lagoon volume in m^3 obtained for each event from 2.91m of water-level in the lagoon until the opening level versus accumulated precipitation for each event with the same timing (black points) and the linear regression (blue line).

Combining equations 4 and 5 we can obtain the relation between the rainfall and the lagoon water-level:

$$(6) L_{wl} = \frac{(1211R_f + 820018)}{259641}$$

247 To validate this relation, we have used the values of rainfall in our study area and the recorded lagoon
 248 water-levels. Figure 4 represents the L_{wl} , recorded and predicted using equation 6, at the barrier breach. The
 249 predicted values are close to the recorded values (less than 0.3 m of difference) with the exception of the events
 250 2 and 3, having a difference of 0.5 and 0.8 m respectively.

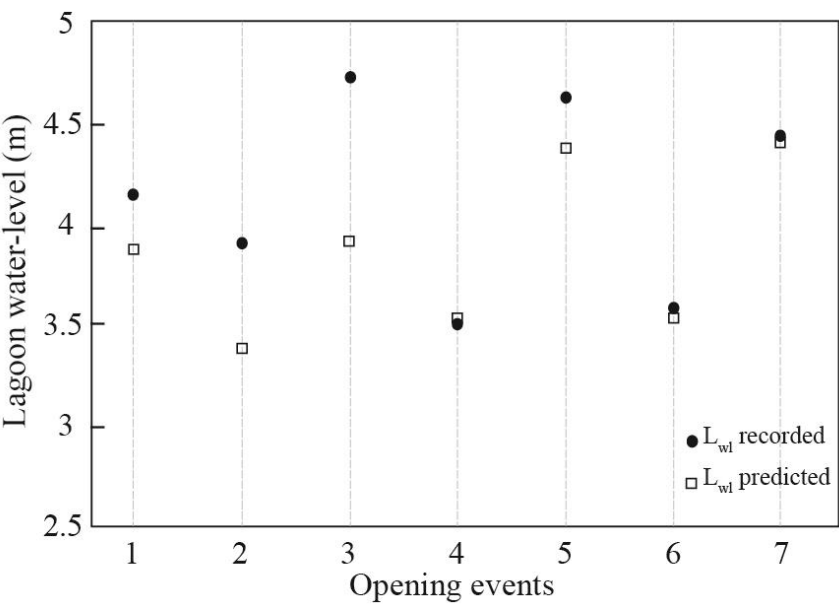


Figure 4. Lagoon water-level in m for each opening event. Black points represent the recorded water-levels and the grey points the predicted water-levels using the equation 6.

251

252 4.3. Nearshore water-levels

253 Figure 2A shows the complete record of sea level during the monitoring program. The mean sea water-
 254 level (MW) was 1.99 m above MSLA; close to the basal level recorded in the lagoon (i.e. 2 m). The obtained
 255 mean low water-level (MLW) was 0.19 m while the mean high water-level (MHW) was 3.83 m above MSLA.
 256 However, sea level reached values of 4.4 m during storm events (Figure 2A). Identified openings occurred at
 257 spring tides or close to spring tides with the exception of opening 7, which took place close to neap tides. Four
 258 of the recorded openings occurred close to the high tide (openings 1, 3, 4 and 6) while the other three (opening
 259 2, 5 and 7) happened close to the low tide (Table 2).

260 Figures 2C, D and E show the wave parameters obtained from the node SIMAR-3009017 and the
 261 propagated waves with SWAN model at points 1 and 2 (Figure 1). The results show that higher wave heights
 262 came from SW, suggesting the occurrence of storms recorded during the wet seasons. Waves from SW impact
 263 the beach directly while waves from westerly and northerly directions are transformed before reaching the

264 beach due to wave refraction. The effect of refraction is not linear and becomes higher as the offshore waves
265 approach NW, reaching a maximum difference of 50° between offshore and local wave direction (e.g. 343° -
266 NNW- transformed to 290°-WNW-). The wave height and period were reduced by 30% and 20% respectively.
267 Differences between the nearshore points 1 and 2 were only observed on waves above 3m, suggesting a higher
268 effect as the waves enter the northern-end of the bay.

269 The minimum and maximum values estimated for barrier elevation (B_{hmin} and B_{hmax}) before the openings
270 are presented in Table 2, ranging from 3.7 to 5.3 m. The latter were associated with local waves arriving
271 parallel to the beach or with low angles (≈ 225 - 230°) and high periods (>8 s), promoting onshore sediment
272 transport.

273 In the same way, B_{wl} at the openings were calculated and are presented in Table 2. The estimated values of
274 B_{wl} for four of the identified openings were lower than the recorded L_{wl} (openings 2, 3, 5 and 7), resulting in a
275 positive water-head difference. Alternatively, the other three cases estimated B_{wl} values were higher than L_{wl}
276 (openings 1, 4 and 6), producing a negative water-head difference (Table 2).

277 4.4. Processes and data integration

278 Barrier breaching was tentatively parameterized using the relation between the L_{wl} (lagoon water-level); B_h
279 (Barrier height) and B_{wl} (barrier water-level). Wave climate, rainfall and the tidal range modulate the selected
280 parameters. Indeed, the water level in the lagoon can be predicted using the accumulated rainfall, while the
281 elevation of the berm can be estimated using the local wave climate and nearshore water level. In addition, the
282 relation between these parameters determines the mechanism that will induce barrier breaching and could be
283 used to predict the timing, the direction of the lagoon openings and, therefore, the type of opening. Three types
284 of openings have been identified: (i) *Lw-type* or breaching triggered from the lagoon, (ii) *Sw-type* or breaching
285 triggered from the sea and (iii) *Mx-type* or mixed lagoon-sea opening.

286 (i) *Lw-type*. Three of the identified events were included into this type of event: openings 3, 5 and
287 7 (Figure 5, event 5). *Lw-type* was associated with the highest recorded water-levels in the lagoon,
288 ranging from 4.43 to 4.72 m, and highest values of accumulated rainfall with values up to
289 268.5 l/m^2 . The high lagoon water-levels were maintained between 21.8 and 61.2 hours, what we
290 have named as the plateau phase (Table 2). This type was also associated with a strong barrier,
291 with more than 48 days to recover from a previous opening (Table 2). In addition, the water-head

difference (Table 2), always showed positive values greater than 1 m, generating a gradient between the lagoon and the sea side. *Lw-types* were preferably happening with low waves heights and spring tide, only the event 7 occurred with high height waves but at low and close to neap tides (Table 2). We observed that for all these cases the relation $L_{wl} \geq B_{hmin} > B_{wl}$ was filled.

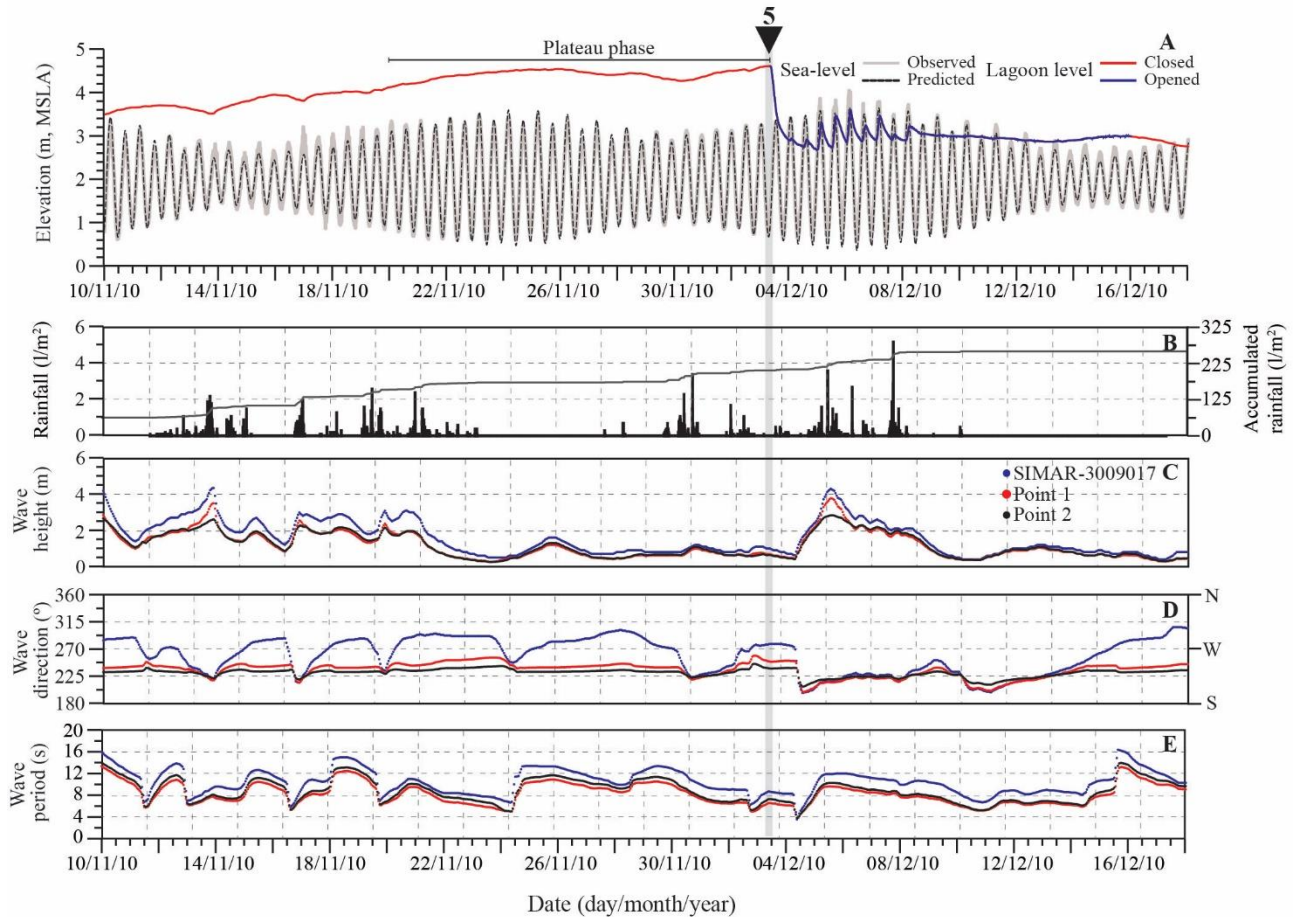


Figure 5. Example of *Lw type* (event 5). (A) lagoon water-level and sea-level, (B) rainfall and (C, D, E) waves previous, during and after the opening..

- (ii) *Sw-type*. Openings 4 and 6 (Figure 6, event 4) were classified as *Sw-type*. In both cases, the opening occurred shortly after beach berm reconstruction, following barrier breaching within the same wet period. The water-level inside the lagoon and the accumulated rainfall was lower than for the *Lw-type*, with values circa 3.5 m of water-level and circa 80 l/m² for rainfall (Table 2). Estimated beach berm elevations before the opening were similar or lower than the values obtained for the *Lw-type* (see Table 2). However, the barrier recovery time in these cases was less than 20 days (Table 2), and the SW waves reached the beach at an oblique angle to the shoreline.

These waves were previously documented as responsible for the beach-face erosion in the study area, provoking the lowering and narrowing of the barrier (Almécija et al., 2009). Water-head differences were negative and greater than 1 m for these cases, generating an inverse gradient between the lagoon and the ocean. During these events, the plateau phase was not present. *Sw type* events developed during spring tides, coincident with high tides and high SW waves promoting high runup values (see Figure 2 and Table 2). For these cases the observed relation between the three variables was $B_{wl} \geq B_{hmax} > L_{wl}$.

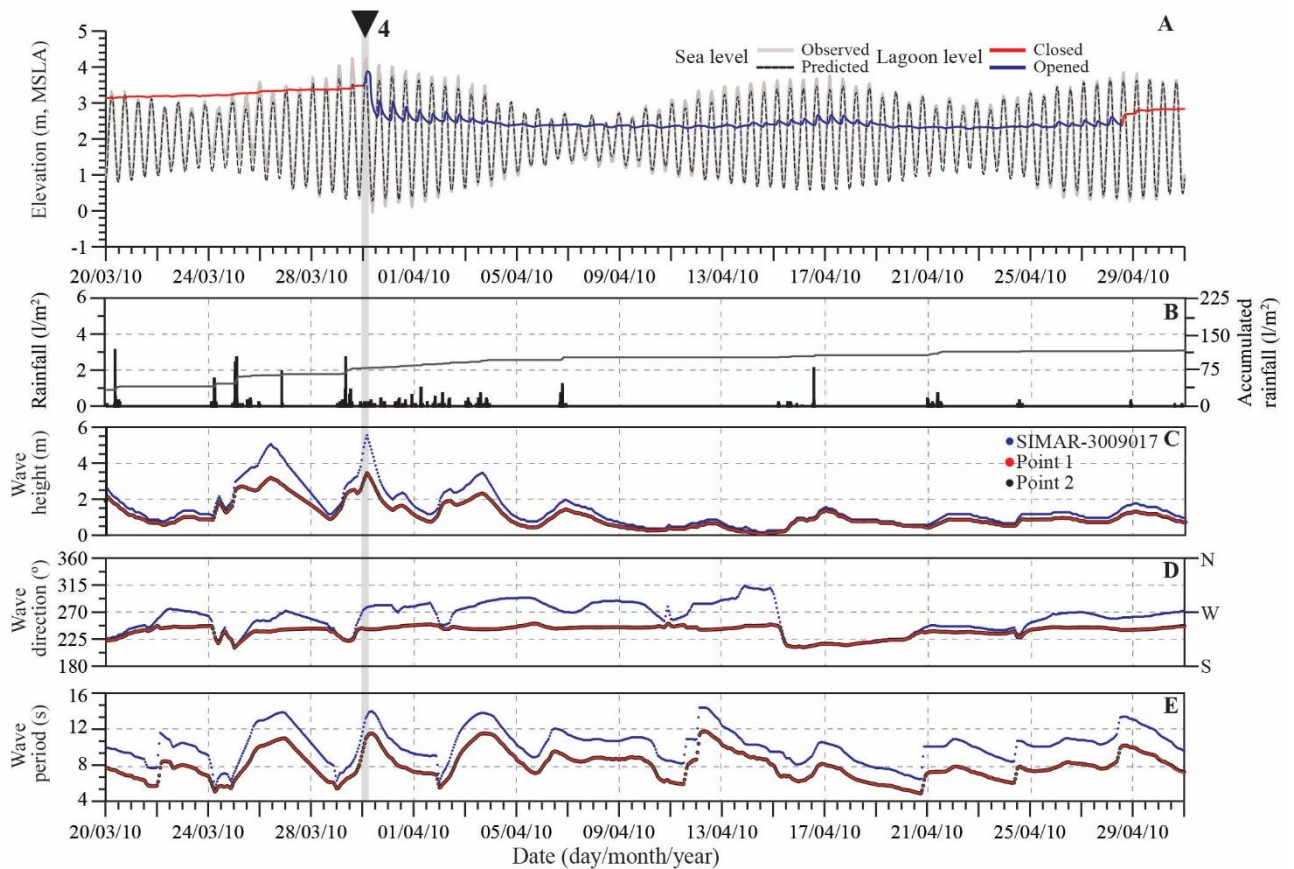


Figure 6. Example of *Sw type* (event 4). (A) lagoon water-level and sea-level, (B) rainfall and (C, D, E) waves, previous, during and after the opening.

- (iii) *Mx-type*. This type represents the openings 1 and 2 (Figure 7, event 2) that could not be easily grouped within the *Lw-* and *Sw-types*. The water-level inside the lagoon was relatively high (around 4 m, Table 2). Yet, the water-head difference in this type was positive or negative but lower than 1 m. Moreover, like in the *Sw type*, the days before the opening were characterized by high SW waves, with high erosion potentials to erode the beach berm, inducing barrier breaching.

Under such conditions, it is expected that the weak barrier would not be able to store high water-volumes in the lagoon, maintaining the plateau phase only for less than 16 hours. For that type of opening, the relation between the variables was $L_{wl} \approx B_{hmin} < \text{or} > B_{wl}$.

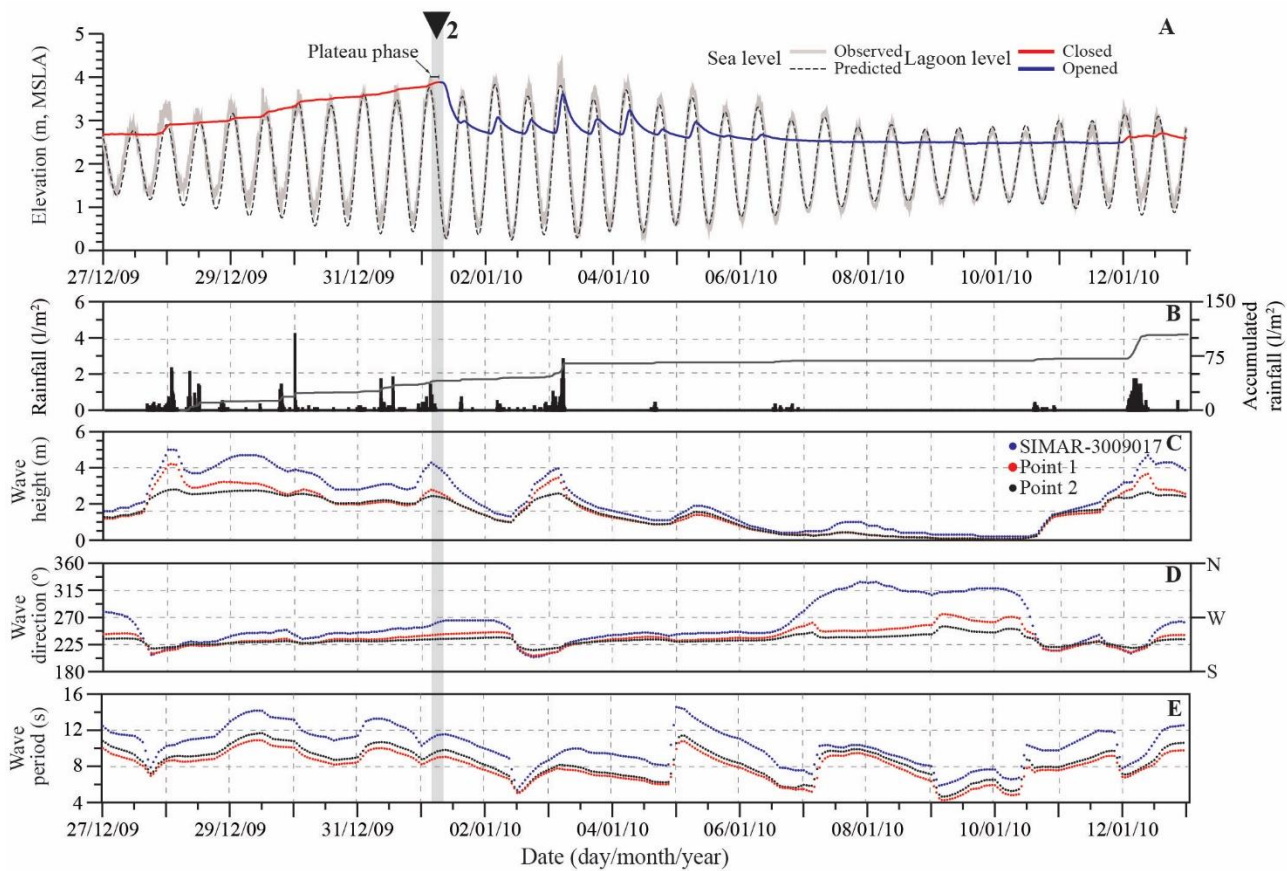


Figure 7. Example of *Mx* type (event 2). (A) lagoon water-level and sea-level, (B) rainfall and (C, D,E) waves previous, at and after the opening.

If the water-levels in the lagoon or at the barrier do not reach the minimal barrier crest height the barrier is not breached, even with high water head differences (event *, Table2). For this cases the situation is defined by $L_{wl} < B_{hmin} > B_{wl}$.

Once open, the lagoon can maintain its direct connection with the open sea for a variable length of time, ranging from 7 to 29 days. The duration of this phase does not show a clear relation with the lagoon water-level (Table 2). In turn, inlet longevity at Louro seems to be regulated by the rainfall regime and wave climate after the opening. The identified closure events were coincident with a cessation of rain, which would explain the reduction of the water input, and the incidence of constructive waves characterized by higher period values. The latter would promote the onshore sediment transport and the development of high berms with the

subsequent barrier growth and widening. In some cases, barrier sealing was interrupted by high erosive waves, and a slight amount of rainfall; this was observed clearly in opening 2 and 4 (Early-January 2010-Figure 7- and Mid-April 2010- Figure 6).

5. DISCUSSION

The ultimate objective of this work was to monitor water-level oscillations within an intermittently open coastal lagoon and the adjacent nearshore, providing a continuous medium-term (> 2 years), high temporal resolution record of water-level oscillations to understand natural breaching processes and evaluate the role of the major forcers (i.e. rainfall regime or wave climate) during these events. The methodology selected to achieve this purpose allowed barrier breaching and closure identification through the occurrence of water-level changes in the lagoon.

One or other of the identified opening types (*Lw*-, *Sw*- and *Mx*-types) have been previously described at other case studies. Yet, in most of the cases, references to breaching processes at lagoons usually focus on one of these types, suggesting a persistent relation between sites and types of opening; i.e. openings from the lagoon side (Joseph, 1958; Kraus et al., 2008; Rich and Keller, 2013; Rijkenberg, 2015), which are comparable to our *Lw*-type, versus breaching induced by high waves (Penland and Suter, 2011; Pierce, 1970; Vidal-Juárez et al., 2014), comparable to our *Sw*-type. All examples found in the literature suggest common processes to explain barrier breaching with independence of site-specific features such as catchment area or lagoon basin dimensions.

At Louro, barrier breaching induced from the land side (lagoon) results from water-level rise in the lagoon as a consequence of intense rainfall and river discharges, in this case under torrential regime. The natural breaching occurs when $L_{wl} \geq B_{hmin} > B_{wl}$ and after the high lagoon water-levels are maintained for a long period of time, and the water-head value is above 1 m. Under these circumstances we may expect two processes leading barrier breaching as described by Kraus and Wamsley (2003): (i) overflow from the lagoon side, and (ii) seaward seepage generated by the groundwater gradient associated to the difference in water elevation between the both sides of the barrier, contributing to liquefaction and removal of the barrier sand. The estimated berm elevations suggest that a combination of both processes should lead to barrier breaching in Louro. In fact, we have found that barrier breaching in *Lw*- and *Mx*-types, only occurs when the water-level in the lagoon equals or exceeds the minimum estimated barrier elevation, which in turn maximizes the potential

358 seepage to compensate the generated gradient of water elevation between the lagoon and the sea side of the
359 barrier. Indeed, the event observed in February 2011 (event *, Figure 2), despite a clear positive and large
360 water head difference, did not lead to an opening because recorded L_{wl} were below B_{hmin} and therefore did not
361 triggered a lagoon overflow.

362 Breaching processes generated by overflow from the lagoon have been previously documented along the
363 Californian coast (Joseph, 1958; Kraus et al., 2002), the southeast coast of Australia (Gordon, 1990;
364 Rijkenberg, 2015), the south of Brazil (Figueiredo et al., 2007) and along the southeast African coast (Smith
365 et al., 2014; Zietsman, 2004). For all those cases, high and wide barriers were described, usually backed by
366 lagoons of variable sizes, with the exception of the examples at the southeast African coast, which correspond
367 to narrow estuarine beaches, developed at the mouth of small rivers. Alternatively, breaching processes
368 generated by sediment liquefaction have been usually observed at low and narrow barriers due to the high
369 water-level of the groundwater (Kraus and Wamsley, 2003; Pierce, 1970).

370 Conversely, openings induced from the sea side of the barrier (*Sw-Type*) were linked to high values of wave
371 setup and runup, which in turn contributed to the inundation of the weaker or lower areas of the barrier and
372 subsequent barrier breaching. This type of breaching is more frequently observed and is associated to low
373 barrier islands and low lying barrier spits (Gordon, 1990; Kraus et al., 2002; Kraus and Wamsley, 2003;
374 Penland and Suter, 2011; Pierce, 1970; Vidal-Juárez et al., 2014). In fact, *Sw-type* have been identified when
375 $B_{wl} \geq B_{hmax} > L_{wl}$ and overwash appears to trigger the breaching through the inundation of a barrier section
376 with lower topography, while the impact of the waves increased sediment mobilization and barrier erosion.
377 The recorded SW waves in this type of opening can generate high runup values, which in turn suggest the
378 onset of inundation regimes during the openings as suggested by the application of the storm impact scale
379 classification proposed by Sallenger (2000). A similar situation occurs when $L_{wl} \approx B_{hmin} < B_{wl}$ (*Mx-type*
380 breaching, opening 1). However, the values of runup for this case did not exceed the estimated B_{hmax} and thus,
381 cannot explain barrier breaching by itself, suggesting the combined effect of waves weakening the barrier and
382 the similar values of water-level in the lagoon side and the B_{hmin} . In addition we can expect that the seaward
383 seepage could contribute to a great extent to barrier breaching also to the latter breaching type, if generated
384 groundwater gradients are considered for all cases. Indeed, a recent experimental work by Turner et al. (2016)
385 had proved how seaward seepage fluxes can be generated under different circumstances, which in turn are

386 coincident with the ones exemplified by *Lw*-, *Sw*- and *Mx*- breaching types.

387 The above suggests that Louro lagoon mimics breaching processes identified worldwide. However, we
388 have also found specific differences that should be highlighted. Revised literature, dealing with openings
389 driven from the lagoon side of the barrier, relate the timing of barrier breaching to low tides, when the water-
390 head difference is largest (Kraus et al., 2008; Rich and Keller, 2013; Rijkenberg, 2015). However, at Louro
391 this type of breaching seems to occur when the hydraulic gradient lagoon-sea is positive, independently of the
392 tidal elevation; *Lw-type* openings occurred close to the high, close to low or in low tide. In addition, it is worth
393 noticing that our case is one of the few showing natural, instead of human-induced, breaching. The latter is
394 usually provoked at low tides to maximize lagoon drainage and avoid hinterland flooding. Other point to
395 highlight is the fact that our records indicate that *Lw-type* only happens when the high water-level inside the
396 lagoon is maintained over time (long plateau phase), yet the actual breaching occurs only if the values of water-
397 head difference are above 1 m. Other examples described in the literature stated that the influence of the water-
398 head difference is more important than the forcing for the actual rain (Rijkenberg, 2015), but in our case the
399 torrential nature of the river provokes that the water-head is directly due to the persistence of rainfall. Indeed,
400 the water-level records at Louro suggest that the greatest water-head differences only provoke barrier
401 breaching if the rain extends time enough to ensure barrier overflow from the lagoon. Per contra, if rainfall
402 stops the barrier might not be saturated and therefore breaching might be prevented (see event *, Figure 2 and
403 Table 2).

404 As stated in the results, the lagoon can maintain its connection with the open sea for a variable period of
405 time. However, this study contrast with previous works concluding that growing and stability of the channel
406 from the lagoon side mainly depends on the strength of the ebb-flow created by the volume of water stored
407 within the lagoon prior to openings (Cruces et al., 2009; Fortunato et al., 2014; Stretch and Parkinson, 2006).
408 This response is not observed in Louro, where the lifespan of the inlet seems to depend on the rainfall regime
409 and the wave climate. Sealing processes dominated by wave climate have been reported at other sites (Costas
410 et al., 2005; Dodet et al., 2013; Fortunato et al., 2014; Kraus et al., 2008). However, in those examples the
411 actual conditions promoting the closure are not clearly explained; it is simplified as a natural trend to close by
412 wave driven sediment transport when the outflow is sufficiently reduced. In this regard, it has been suggested
413 that inlet closure is at a great extent promoted by the onshore or longshore transport of the sediment originally

414 ejected by the breaching. The role of the onshore transport was also described in the closure of seasonally open
415 small tidal inlets by Ranasinghe and Pattiaratchi (2003) who demonstrated that onshore transport of material
416 can induce closure if the longshore sediment transport rate is small or inadequate.

417 Finally, we have explored the relation between the number of openings per year and the corresponding
418 local climate (Figure 2), finding that the number of openings decreased (increased) with the decreased
419 (increase) of the annual rainfall and with the decreased (increased) occurrence of erosive high and SW waves.
420 Climate projections for the Western Iberian region predict an upward trend of the NAO towards more positive
421 values and a greater frequency of warm and dry winters in the future (López-Moreno et al., 2011), leading to
422 a significant decline of the annual precipitation (Sáez de Cámara et al., 2015; Trigo et al., 2004; Trigo et al.,
423 2008). Water-level monitoring at Louro provides supporting evidences that the lagoon waters may not be
424 renewed if rainfall is low or highly intermittent. If so, the system functionality may be negatively affected due
425 to the eutrophication, as water renewal can be dramatically reduced. Previous works documented that artificial
426 actions (barrier breaching) avoid or mitigate this situation enhancing system functionality (del Barrio
427 Fernández et al., 2012; Smith, 2003). However, if these actions are not well addressed the consequences for
428 the lagoons can be negative instead (De Decker, 1987; Dye and Barros, 2005; Netto et al., 2012). The present
429 work shows an example on how a monitoring program may contribute to the implementation of appropriate
430 management practices, through the definition of the relation between the principal variables governing barrier-
431 breaching processes under changing environmental conditions.

432

433 6. CONCLUSIONS

434 In this work we present a monitoring program of water-level oscillations within Louro lagoon, a small
435 coastal lagoon, included in the Natura 2000 network of the EU, based on the analysis of a dataset expanding
436 more than 2 years. The monitoring included water-level observations in the lagoon and seaward. These datasets
437 are useful to locate accurately the opening timing and to establish the variables playing at breaching time with
438 climatic, wave and topographic data. The methodology proposed in this paper allows us to understand this
439 process at medium-term time scales. However, the co-occurrence of climate related processes (such as heavy
440 rainfall or sea storms) adds uncertainty in the identification of drivers during breaching. To account for those
441 uncertainties, we have first identified the events and then used additional data; i.e. topography, wave

parameters and rainfall to parametrize the variables responsible for lagoon opening.

We can parametrize three principal variables responsible for triggering the natural openings: L_{wl} , lagoon water-level; B_h , barrier height and B_{wl} , beach water-level.

We found that each variable is dependent of other processes, in that way, the L_{wl} is highly modulated by the rainfall regime, B_h is dependent of the wave climate (runup) and the B_{wl} depends on the tidal regime (tidal height) and wave climate (runup).

Three types of openings were identified in function of the relation between these three variables:

- *Lw-type*, when $L_{wl} \geq B_{hmin} > B_{wl}$; opening from the lagoon side, by lagoon water overflow.
- *Sw-type*; when $B_{wl} \geq B_{hmax} > L_{wl}$; opening from the sea side, by wave overwash or lagoon inundation
- *Mx-type*; when $L_{wl} \approx B_{hmin} < \text{or} > B_{wl}$; the opening is triggered by a combination of processes from both sides.

However, when $L_{wl} < B_{hmin} > B_{wl}$; there is no opening.

The natural openings are climate modulated, indeed the occurrence of the natural openings are linked to rainfall regimes. The results suggest that if the projections are right, the study area will tend to register more frequent warm and dry winters, which in turn will lead to a decrease on the annual precipitation and thus a reduction on the communication of the lagoon with the open sea. The latter has negative consequences over the lagoon ecosystem due to the reduction of its functionality.

With this work we prove that understanding how and when a lagoon opens naturally is possible and that it can support and improve management practices. On the other hand, the quality and temporal extent of the dataset provides a perfect framework for future work, which should include model calibration of opening and closure processes.

7. ACKNOWLEDGEMENTS

Financial support was provided by grants from the Xunta de Galicia (08MDS036000PR) and MICINN (CTM2012-39599-C03-01). The authors would like to thank Puertos del Estado (Ministerio de Fomento) for the SIMAR-44 database provided for this study and to the IGN (© Instituto Geográfico Nacional de España), for providing the LiDAR data and aerial imagery. We thank the Regional Weather Forecast Agency

469 (MeteoGalicia) for kindly providing the climatic data. We also thank the members of the XM-1 group (U.
470 Vigo) for field assistance. R. González-Villanueva was funded by the Xunta de Galicia Post-Doc Fellowship
471 (PlanI2C-ED481B 2014/132-0). Susana Costas was founded by the Portuguese Science Foundation through
472 the “FCT Investigator” program (ref. IF/01047/2014).

473 8. REFERENCES

- 474 Almécija, C., 2009. Morfodinámica e hidrodinámica de una playa expuesta. Ejemplo de la playa de louro
475 (muros, nw península ibérica). Master Thesis Thesis, Universidad de Vigo, Vigo, 54 pp.
- 476 Almécija, C., Villaceros-Robineau, N., Alejo, I. and Pérez-Arlucea, M., 2009. Morphodynamic conceptual
477 model of an exposed beach: The case of louro beach (galicia, nw, iberia). *Journal of Coastal Research*,
478 SI 56: 1711-1715.
- 479 Battjes, J.A., 1974. Surf similarity. 14th Conference of Coastal Engineering, p.^pp. 466-480.
- 480 Bird, E.C.F., 1993. Physical setting and geomorphology of coastal lagoons. In: B. Kjerfve (Editor), *Coastal*
481 *lagoon processes*. Elsevier, Amsterdam, pp. 9–39.
- 482 Booij, N., Ris, R.C. and Holthuijsen, L.H., 1999. A third-generation wave model for coastal regions: 1. Model
483 description and validation. *Journal of Geophysical Research: Oceans*, 104(C4): 7649-7666.
- 484 Boon, J.D., 2004. *Secrets of the tide : Tide and tidal current analysis and applications, storm surges and sea*
485 *level trends*. Horwood Pub., Chichester, U.K.
- 486 Boothroyd, J., 1985. Tidal inlets and tidal deltas. In: R. Davis, Jr. (Editor), *Coastal sedimentary environments*.
487 Springer New York, pp. 445-532.
- 488 Castelle, B. et al., 2007. Dynamics of a wave-dominated tidal inlet and influence on adjacent beaches,
489 currumbin creek, gold coast, australia. *Coastal Engineering*, 54(1): 77-90.
- 490 Cayocca, F., 2001. Long-term morphological modeling of a tidal inlet: The arcachon basin, france. *Coastal*
491 *Engineering*, 42(2): 115-142.
- 492 Cobelo-García, A. et al., 2012. Temporal and diel cycling of nutrients in a barrier–lagoon complex:
493 Implications for phytoplankton abundance and composition. *Estuarine, Coastal and Shelf Science*,
494 110(0): 69-76.
- 495 Costas, S., Alejo, I., Vila-Concejo, A. and Nombela, M.A., 2005. Persistence of storm-induced morphology
496 on a modal low-energy beach: A case study from nw-iberian peninsula. *Marine Geology*, 224: 43-56.
- 497 Cruces, A., Freitas, M.C. and Andrade, C., 2009. Morphodynamics of the artificial inlet of santo andré coastal
498 lagoon (sw portugal) - twelve years of monitoring. In: G. Flor Rodríguez, J. Gallastegui, G. Flor
499 Blanco and J. Martín LLaneza (Editors), 6º Simposio sobre el Margen Ibérico Atlántico MIA09,
500 Oviedo, pp. 233-236.
- 501 De Decker, H.P., 1987. Breaching the mouth of the bot river estuary, south africa: Impact on its benthic
502 macrofaunal communities. *Transactions of the Royal Society of South Africa*, 46(3): 231-250.
- 503 del Barrio Fernández, P., Gómez, A.G., Alba, J.G., Díaz, C.Á. and Revilla Cortezón, J.A., 2012. A model for
504 describing the eutrophication in a heavily regulated coastal lagoon. Application to the albufera of
505 valencia (spain). *Journal of Environmental Management*, 112(0): 340-352.
- 506 Dodet, G. et al., 2013. Wave-current interactions in a wave-dominated tidal inlet. *Journal of Geophysical*
507 *Research: Oceans*, 118(3): 1587-1605.
- 508 Dussaillant, A., Galdames, P. and Sun, C.-L., 2009. Water level fluctuations in a coastal lagoon: El yali ramsar
509 wetland, chile. *Desalination*, 246(1-3): 202-214.
- 510 Dye, A. and Barros, F., 2005. Spatial patterns of macrofaunal assemblages in intermittently closed/open coastal
511 lakes in new south wales, australia. *Estuarine, Coastal and Shelf Science*, 64(2–3): 357-371.
- 512 Fagherazzi, S. and Priestas, A.M., 2012. Back-barrier flooding by storm surges and overland flow. *Earth*
513 *Surface Processes and Landforms*, 37(4): 400-410.
- 514 Figueiredo, S.A., Cowell, P. and Short, A., 2007. Intermittent backbeach discharge to the surfzone: Modes and
515 geomorphologic implications. *Journal of Coastal Research*, SI 50: 4.
- 516 FitzGerald, D.M., Kraus, N.C. and Hands, E.B., 2000. Natural mechanisms of sediment bypassing at tidal
517 inlets, US Army Corps of Engineers.
- 518 Fitzgerald, D.M., Penland, S. and Nummedal, D., 1984. Control of barrier island shape by inlet sediment

519 bypassing: East frisian islands, west germany. In: B. Greenwood and R.A. Davis (Editors),
520 Developments in sedimentology. Elsevier, pp. 355-376.

521 Fortunato, A.B. et al., 2014. Morphological evolution of an ephemeral tidal inlet from opening to closure: The
522 albufeira inlet, portugal. *Continental Shelf Research*, 73(0): 49-63.

523 Gale, E., Pattiaratchi, C. and Ranasinghe, R., 2006. Vertical mixing processes in intermittently closed and open
524 lakes and lagoons, and the dissolved oxygen response. *Estuarine, Coastal and Shelf Science*, 69(1-2):
525 205-216.

526 González-Villanueva, R., 2013. Origin, evolution and processes controlling holocene barrier-lagoon systems
527 (nw spain), Universidad de Vigo, 199 pp.

528 Goodess, C.M. and Jones, P.D., 2002. Links between circulation and changes in the characteristics of iberian
529 rainfall. *International Journal of Climatology*, 22(13): 1593-1615.

530 Gordon, A.D., 1981. Behaviour of lagoon inlets. National Conference Publication - Institution of Engineers,
531 Australia, p.^pp. 54-58.

532 Gordon, A.D., 1990. Coastal lagoon entrance dynamics. *Coastal Engineering Proceedings*(22).

533 Green, A., Cooper, J.A.G. and LeVieux, A., 2013. Unusual barrier/inlet behaviour associated with active
534 coastal progradation and river-dominated estuaries. *Journal of Coastal Research*: 35-45.

535 Hayes, M.O., 1979. Barrier islands morphology as a function of tidal and wave regime. In: S.P. Leatherman
536 (Editor), *Barrier islands from the gulf of st. Lawrence to the gulf od mexico*. Academic Press, New
537 York, pp. 1- 27.

538 Joseph, J., 1958. Studies of big lagoon, humboldt county, california 1956-1958. Master Thesis Thesis,
539 Humboldt State University, Humboldt, California, 137 pp.

540 Kraus, N.C., Militello, A. and Todoroff, G., 2002. Barrier breaching processes and barrier spit breach, stone
541 lagoon california. *Shore & Beach*, 70(4): 8.

542 Kraus, N.C., Munger, S. and Patsch, K., 2008. Barrier beach breaching from the lagoon side, with reference to
543 northern california. *Shore & Beach*, 2(76): 10.

544 Kraus, N.C. and Wamsley, T.V., 2003. Coastal barrier breaching. Part 1: Overview of breaching processes,
545 U.S. Army Engineer Research and Development Center, Vicksburg, MS.

546 López-Moreno, J.I. et al., 2011. Effects of the north atlantic oscillation (nao) on combined temperature and
547 precipitation winter modes in the mediterranean mountains: Observed relationships and projections
548 for the 21st century. *Global and Planetary Change*, 77(1-2): 62-76.

549 Martínez Cortizas, A. and Pérez Alberti, A., 1999. Atlas climático de galicia, Xunta de Galicia, 207 pp.

550 Moreno, I.M., Ávila, A. and Losada, M.Á., 2010. Morphodynamics of intermittent coastal lagoons in southern
551 spain: Zahara de los atunes. *Geomorphology*, 121(3-4): 305-316.

552 Morris, B.D. and Turner, I.L., 2010. Morphodynamics of intermittently open-closed coastal lagoon entrances:
553 New insights and a conceptual model. *Marine Geology*, 271(1-2): 55-66.

554 Netto, S.A., Domingos, A.M. and Kurtz, M.N., 2012. Effects of artificial breaching of a temporarily
555 open/closed estuary on benthic macroinvertebrates (camacho lagoon, southern brazil). *Estuaries and*
556 *Coasts*, 35(4): 1069-1081.

557 Osborn, T.J., Briffa, K.R., Tett, S.F.B., Jones, P.D. and Trigo, R.M., 1999. Evaluation of the north atlantic
558 oscillation as simulated by a coupled climate model. *Climate Dynamics*, 15(9): 685-702.

559 Pacheco, A., Ferreira, Ó. and Williams, J.J., 2011. Long-term morphological impacts of the opening of a new
560 inlet on a multiple inlet system. *Earth Surface Processes and Landforms*, 36(13): 1726-1735.

561 Penland, S. and Suter, J.R., 2011. Low-profile barrier islands overwash and breaching in the gulf of mexico.
562 *Coastal Engineering Proceedings*(19).

563 Pérez-Arlucea, M., Alméjida, C., González-Villanueva, R. and Alejo, I., 2011. Water dynamics in a barrier-
564 lagoon system: Controlling factors. *Journal of Coastal Research*(SI 64): 15-19.

565 Pierce, J.W., 1970. Tidal inlets and washover fans. *The Journal of Geology*, 78(2): 230-234.

566 Ranasinghe, R. and Pattiaratchi, C., 2003. The seasonal closure of tidal inlets: Causes and effects. *Coastal*
567 *Engineering Journal*, 45(04): 601-627.

568 Ranasinghe, R., Pattiaratchi, C. and Masselink, G., 1999. A morphodynamic model to simulate the seasonal
569 closure of tidal inlets. *Coastal Engineering*, 37(1): 1-36.

570 Rich, A. and Keller, E.A., 2013. A hydrologic and geomorphic model of estuary breaching and closure.
571 *Geomorphology*, 191: 64-74.

572 Rijkenberg, L., 2015. Wave-dominated tidal inlet systems: Processes which force opening and closure of
573 intermittently open natural inlets. Master Thesis, Delft University of Technology, 152 pp.

574 Rodriguez-Fonseca, B. and de Castro, M., 2002. On the connection between winter anomalous precipitation
575 in the iberian peninsula and north west africa and the summer subtropical atlantic sea surface
576 temperature. *Geophysical Research Letters*, 29(18): 1863.

577 Roy, P.S. et al., 2001. Structure and function of south-east australian estuaries. *Estuarine, Coastal and Shelf*
578 *Science*, 53(3): 351-384.

579 Sáez de Cámara, E., Gangoiti, G., Alonso, L. and Iza, J., 2015. Daily precipitation in northern iberia:
580 Understanding the recent changes after the circulation variability in the north atlantic sector. *Journal*
581 *of Geophysical Research: Atmospheres*, 120(19): 9981-10,005.

582 Sallenger, A.H., Jr., 2000. Storm impact scale for barrier islands. *Journal of Coastal Research*, 16(3): 890-895.

583 Schallenberg, M., Larned, S.T., Hayward, S. and Arbuckle, C., 2010. Contrasting effects of managed opening
584 regimes on water quality in two intermittently closed and open coastal lakes. *Estuarine, Coastal and*
585 *Shelf Science*, 86(4): 587-597.

586 Smith, A.M., Guastella, L.A. and Goble, B.J., 2014. Forecasting lagoon outlet erosion: Kwazulu-natal,
587 southeast africa. *Journal of Coastal Research*: 151-155.

588 Smith, V., 2003. Eutrophication of freshwater and coastal marine ecosystems a global problem. *Environ Sci*
589 *& Pollut Res*, 10(2): 126-139.

590 Stockdon, H.F., Holman, R.A., Howd, P.A. and Sallenger Jr, A.H., 2006. Empirical parameterization of setup,
591 swash, and runup. *Coastal Engineering*, 53(7): 573-588.

592 Stretch, D. and Parkinson, M., 2006. The breaching of sand barriers at perched, temporary open-closed estuaries
593 - a model study. *Coastal Engineering Journal*, 48(01): 13-30.

594 Trigo, R.M. et al., 2004. North atlantic oscillation influence on precipitation, river flow and water resources in
595 the iberian peninsula. *International Journal of Climatology*, 24(8): 925-944.

596 Trigo, R.M. et al., 2008. The impact of north atlantic wind and cyclone trends on european precipitation and
597 significant wave height in the atlantic. *Annals of the New York Academy of Sciences*, 1146(1): 212-
598 234.

599 Turner, I.L., Rau, G.C., Austin, M.J. and Andersen, M.S., 2016. Groundwater fluxes and flow paths within
600 coastal barriers: Observations from a large-scale laboratory experiment (bardex ii). *Coastal*
601 *Engineering*, 113: 104-116.

602 Vidal-Juárez, T., Ruiz de Alegría-Arzaburu, A., Mejía-Trejo, A., García-Nava, H. and Enríquez, C., 2014.
603 Predicting barrier beach breaching due to extreme water levels at san quntín, baja california, mexico.
604 *Journal of Coastal Research*: 100-106.

605 Wainwright, D.J. and Baldock, T.E., 2015. Measurement and modelling of an artificial coastal lagoon breach.
606 *Coastal Engineering*, 101: 1-16.

607 Weidman, C.R. and Ebert, J.R., 2013. Cyclic spit morphology in a developing inlet system, Formation and
608 evolution of multiple tidal inlets. *American Geophysical Union*, pp. 186-212.

609 Zietsman, I., 2004. Hydrodynamics of temporary open estuaries, with case studies of mhlanga and mdloti.
610 Master Thesis Thesis, University of Kwa-Zulu Natal, South Africa, 131 pp.